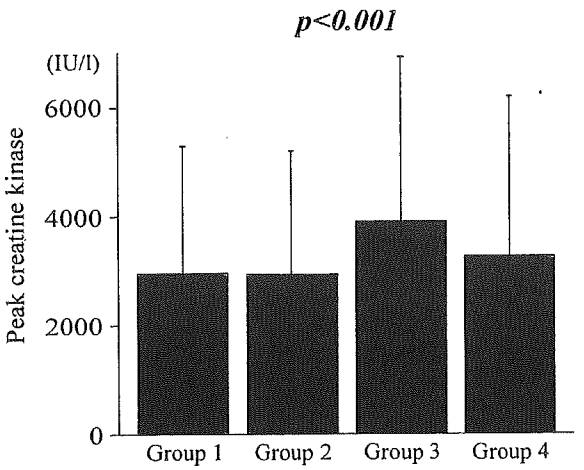

Fig 1. Peak creatine kinase level was higher in group 3, and infarct sizes were similar in the other 3 groups.

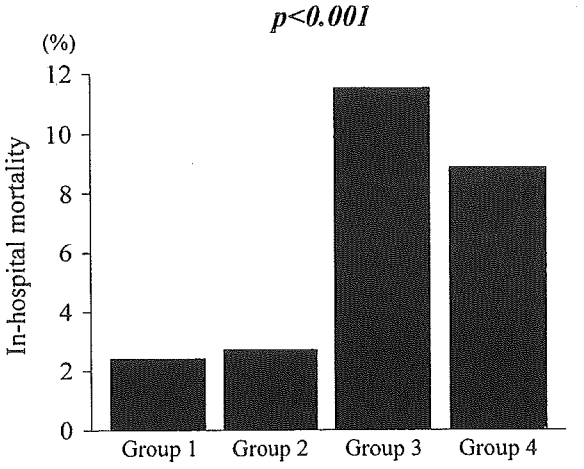

Fig 2. In-hospital mortality was highest in group 3 and second highest in group 4.

Statistical Analysis

Data are expressed as mean values ± standard deviation for continuous variables and as percentages for categorical variables. We made comparisons by one-way analysis of variance for continuous variables, and the statistical significance of differences was calculated by using the Scheffe F test. Chi-squared analysis or Fisher's exact test was used to compare categorical variables. A two-tailed p value of <0.05 was considered to indicate statistical significance. Multiple logistic regression analysis was used to examine determinants of in-hospital mortality. Variables used for analysis included an age of >70 years,[12] sex, time to admission, Killip >1 on admission, previous infarction, serum creatinine level on admission, ST-segment elevation, anterior infarction, absence of previous angina within 24 h before symptom onset, occlusion status at the culprit lesion, 3-vessel disease, stent implantation, final TIMI flow grade ≤2, and glycemic status. The strength of association of glycemic status was assessed by comparison of the 3 groups with a disordered blood glucose profile to the normal (group 1) patients who had no diagnosis of diabetes without admission hyperglycemia. Analyses were conducted with the use of SPSS PC software.

Results

Patient Characteristics

The overall prevalence of diabetes in the study group was 30%. Patients' characteristics in the 4 study subgroups are presented in Table 1. Non-diabetic patients with admission hyperglycemia were likely to be oldest. Patients with admission hyperglycemia were likely to be female and to be in the Killip class >1 on admission, and independent of a diabetic status. The prevalence of previous infarction was slightly but not significantly higher in the diabetic patients than in the non-diabetic patients. Diabetic patients with admission hyperglycemia had the highest blood glucose level on admission and the highest HbA1c value. In general, diabetic patients were more likely to have hyperlipidemia and hypertension than non-diabetic patients. Diabetic patients were more likely to be receiving aspirin, angiotensin-converting enzyme inhibitors, and hydroxymethylglutaryl-coenzyme A reductase inhibitors. There were no differences in the 4 groups with regard to time from symptom onset to admission, infarct location, serum creatinine level on admission, and prevalence of ST-segment elevation.

Coronary Angiographic Findings

The coronary angiographic findings of the patients are presented in Table 1. Stent implantation was performed in 665 patients (78%). Diabetic patients were more likely to have 3-vessel disease than non-diabetic patients. There were no significant differences in the 4 groups with respect to the prevalences of TIMI flow grade 0 at initial coronary angiography, a final TIMI flow grade ≥2, a final TIMI flow grade of 3, or stent implantation.

Peak Creatine Kinase Level

Non-diabetic patients with admission hyperglycemia had a higher peak creatine kinase level than the other 3 groups, which had similar levels (Fig 1).

In-Hospital Mortality

During hospitalization (mean 14 days), 39 patients (4.5%) died (38 of cardiac causes and one of multiple organ failure). In-hospital mortality was higher in non-diabetic and diabetic patients with admission hyperglycemia, especially in the former (Fig 2). Multivariate analysis showed that patients who were >70 years of age, had Killip >1 on admission, serum creatinine on admission, anterior infarction, final TIMI grade ≤2, and admission hyperglycemia, irrespective of the presence or absence of diabetes (groups 3 and 4), were independent predictors of in-hospital death (Table 2).

Discussion

Our findings suggest that in-patients undergoing PCI for AMI, and the presence of admission hyperglycemia with or without diabetes significantly contributed to in-hospital mortality. Diabetes without admission hyperglycemia did not increase in-hospital mortality.

Non-Diabetic Patients With Admission Hyperglycemia

The poor outcome in non-diabetic patients with admission hyperglycemia may arise from a larger infarct size. Hyperglycemia has been shown to increase intercellular adhesion molecule-1, which increases the leukocyte plug-

Table 2 Multivariate Analysis of Factors Associated With In-Hospital Mortality

Variable	*Odds ratio (95%CI)*	*p value*
Group 1	*1.00 (–)*	–
Group 2	*0.80 (0.24–2.60)*	*0.708*
Group 3	*2.29 (1.10–5.49)*	*0.039*
Group 4	*2.14 (1.14–4.69)*	*0.048*
Age >70 years	*3.09 (1.08–9.81)*	*0.049*
Sex	*0.90 (0.32–2.55)*	*0.636*
Time to admission	*1.07 (0.75–1.16)*	*0.519*
Killip >1 on admission	*5.49 (1.88–16.0)*	*0.002*
Previous infarction	*2.49 (0.73–8.45)*	*0.143*
Serum creatinine on admission	*1.82 (1.13–2.93)*	*0.014*
ST-segment elevation	*0.49 (0.11–2.29)*	*0.336*
Anterior infarction	*5.45 (1.68–17.7)*	*0.005*
Absence of previous angina	*1.15 (0.37–3.64)*	*0.280*
TIMI flow grade 0 at initial CAG	*3.67 (0.96–14.0)*	*0.057*
3-vessel disease	*2.93 (0.95–8.98)*	*0.061*
Stent implantation	*1.10 (0.32–3.02)*	*0.976*
Final TIMI flow grade ≤2	*3.53 (1.06–11.7)*	*0.039*

CAG, coronary angiography.
Group 1, Non-diabetic patients without admission hyperglycemia; Group 2, Diabetic patients without admission hyperglycemia; Group 3, Non-diabetic patients with admission hyperglycemia; Group 4, Daibetic patients with admission hyperglycemia.

ging of capillaries[13] augments platelet-dependent thrombus formation[14] and attenuates endothelium-dependent vasodilation[15] Although these mechanisms may contribute to a larger infarct size, we cannot rule out the possibility that hyperglycemia was caused by severe myocardial damage[16] The poor outcome in non-diabetic patients with admission hyperglycemia might also be related to undiagnosed diabetes. Unrecognized diabetes or impaired glucose tolerance may increase endothelial damage due to untreated glucose abnormalities. Two recent studies show that abnormal glucose metabolism is very common in patients with AMI: approximately two-thirds of patients with no previous diagnosis of diabetes have undetected diabetes or impaired glucose tolerance[17,18]

Diabetic Patients With or Without Admission Hyperglycemia

Diabetic patients with admission hyperglycemia had a very high blood glucose level on admission. Nonetheless, these patients had a relatively small infarct size, similar to those in patients without admission hyperglycemia. Diabetic patients with admission hyperglycemia had a higher rate of insulin treatment and a higher HbA1c value, suggesting a longer duration of severe diabetes. Diabetic patients who have impaired islet responses to glucose, especially those with insulin-dependent diabetes, are particularly prone to the development of marked hyperglycemia during stress states[19,20] Marked hyperglycemia in these patients may therefore not correlate with infarct size. However, diabetic patients with admission hyperglycemia had higher in-hospital mortality than did patients in the other groups without admission hyperglycemia. Our findings suggest that the poor outcome in diabetic patients with admission hyperglycemia is primarily related to the deleterious effects of diabetes on myocardial function rather than to infarct size. One explanation is the existence of a specific form of heart muscle disease associated with diabetes. Clinically, this disease manifests itself as left ventricular dysfunction or failure[21] The higher prevalence of Killip class >1 on admission in diabetic patients with admission hyperglycemia, despite a similar infarct size as compared with patients without admission hyperglycemia, may reflect increased susceptibility to the deleterious effects of diabetes. Such effects might be most obvious in patients with a prolonged history of severe diabetes. Hyperglycemia itself may directly impair left ventricular function[6] Furthermore, poorly controlled diabetes may relate to microvascular dysfunction[22] Moreover, coronary atherosclerosis may be more severe and diffuse in diabetic patients with admission hyperglycemia[23] as indicated by the higher incidence of 3-vessel disease. Severer ischemia in the non-infarcted myocardium might increase the risk of heart failure.

Diabetic patients without admission hyperglycemia had a smaller infarct size and a better in-hospital outcome than did patients with admission hyperglycemia, regardless of whether they had a history of diabetes. These findings do not support the results of a recent study by Wahab et al, who showed that diabetic patients, irrespective of admission hyperglycemia, have higher mortality after AMI than non-diabetic patients[6] In-hospital mortality in their diabetic patients was much higher than that in the patients of the present study. These disparate findings may relate to the different treatment strategies used. Patients in the study by Wahab et al, especially those who were diabetic, were less likely to receive thrombolysis or PCI. The worse outcome in their diabetic patients might thus be related, at least in part, to inadequate reperfusion therapy, as suggested previously[6,8] In contrast, we studied only patients who received PCI, and our final success rate was high. The better in-hospital outcome of diabetic patients without admission hyperglycemia in the present study suggests that a higher rate of reperfusion by PCI might improve survival in such patients, compared with that of previous studies. Another important distinction between the 2 studies involves the baseline characteristics of diabetic patients without admission hyperglycemia. In the present study, a smaller proportion of patients were receiving insulin treatment, and the mean HbA1c value was 6.9%, suggesting relatively good glycemic control. Our subjects most likely had milder or a shorter duration of diabetes than those studied by Wahab et al[6] Experimental studies have shown that the heart in the early phase of diabetes is more resistant to ischemia than the non-diabetic heart[24] Another study has reported that a shorter duration of diabetes is associated with a better outcome after AMI[1] These findings suggest that the duration and severity of diabetes are important determinants of outcome.

Study Limitations

This was a retrospective, observational and non-randomized study. However, we included approximately two-thirds of all patients who were admitted to JACSS-affiliated hospitals within 12 h from the onset of AMI. Therefore, we believe that our results serve to demonstrate the effect of glucose abnormalities on in-hospital outcome in patients who receive PCI. In the present study, diabetes mellitus was diagnosed on the basis of whether patients were receiving antidiabetic treatment, blood glucose levels were measured before admission, and the results of oral glucose tolerance tests were available. However, diabetes may have not been diagnosed with the use of these general criteria in some "non-diabetic" patients. The inclusion of such patients may have substantially affected the study results. The inability to exclude such patients from this multicenter retrospective investigation represents an important limitation of our

study design. Nonetheless, the proportion of our subjects who had diabetes (approximately 30%) was consistent with that of previous studies of patients[25] Furthermore, we evaluated infarct size on the basis of peak creatine kinase level, but peak creatine kinase level may not accurately reflect infarct size. Other techniques that allow direct examination of infarct size, such as radioisotopes, are needed to more objectively evaluate infarct size and provide important additional information. Further prospective studies involving larger numbers of patients are required to confirm the effect of admission hyperglycemia for patients on outcome after PCI for AMI.

Conclusions

Our findings suggest that in-patients undergoing PCI for AMI, and admission hyperglycemia, irrespective of the presence or absence of diabetes, is associated with increased in-hospital mortality, whereas diabetes without admission hyperglycemia is not.

Acknowledgments

The authors gratefully acknowledge that the present study was supported by a Research Grant for Cardiovascular Disease (14C-4) from the Ministry of Health, Labour and Welfare.

References

1. Barbash GI, White HD, Modan M, Van de Werf F. Significance of diabetes mellitus in patients with acute myocardial infarction receiving thrombolytic therapy: Investigators of the International Tissue Plasminogen Activator/Streptokinase Mortality Trial. *J Am Coll Cardiol* 1993; **22:** 707–713.
2. Mak KH, Moliterno DJ, Granger CB, Miller DP, White HD, Wilcox RG, et al. Influence of diabetes mellitus on clinical outcome in the thrombolytic era of acute myocardial infarction: GUSTO-I Investigators: Global Utilization of Streptokinase and Tissue Plasminogen Activator for Occluded Coronary Arteries. *J Am Coll Cardiol* 1997; **30:** 171–179.
3. Oswald GA, Corcoran S, Yudkin JS. Prevalence and risk of hyperglycemia and undiagnosed diabetes in patients with acute myocardial infarction. *Lancet* 1984; **1:** 1264–1267.
4. Fava S, Aquilina O, Azzopardi J, Agius Muscat H, Fenech FF. The prognostic value of blood glucose in diabetic patients with acute myocardial infarction. *Diabetic Med* 1996; **13:** 80–83.
5. Capes SE, Hunt D, Malmberg K, Gerstein HC. Stress hyperglycemia and increased risk after myocardial infarction in patients with and without diabetes: A systematic overview. *Lancet* 2000; **355:** 773–778.
6. Wahab NN, Cowden EA, Pearce NJ, Gardner MJ, Merry H, Cox JL, et al. Is blood glucose an independent predictor of mortality in acute myocardial infarction in the thrombolytic era? *J Am Coll Cardiol* 2002; **40:** 1748–1754.
7. Fibrinolytic Therapy Trialists' (FTT) Collaborative Group. Indications for fibrinolytic therapy in suspected acute myocardial infarction: Collaborative overview of early mortality and major morbidity results from all randomised trials of more than 1000 patients. Fibrinolytic Therapy Trialists' (FTT) Collaborative Group. *Lancet* 1994; **343:** 311–322.
8. Pfeffer MA, Moye LA, Braunwald E, Basta L, Brown EJ Jr, Cuddy TE, et al. Selection bias in the use of thrombolytic therapy in acute myocardial infarction: The SAVE Investigators. *JAMA* 1991; **266:** 528–532.
9. Hsu LF, Mak KH, Lau KW, Sim LL, Chan C, Koh TH, et al. Clinical outcomes of patients with diabetes mellitus and acute myocardial infarction treated with primary angioplasty or fibrinolysis. *Heart* 2002; **88:** 260–265.
10. The TIMI study group. The Thrombolysis in Myocardial Infarction (TIMI) trial: Phase I findings. *N Engl J Med* 1985; **312:** 932–936.
11. Report of the Expert Committee on the Diagnosis and Classification of Diabetes Mellitus. American Diabetes Association: Clinical practice recommendation 2002. *Diabetes Care* 2002; **25:** S1–S147.
12. The TIMI Study Group. Comparison of invasive and conservative strategies after treatment with intravenous tissue plasminogen activator in acute myocardial infarction: Results of the thrombolysis in myocardial infarction (TIMI) phase II trial. *N Engl J Med* 1989; **320:** 618–627.
13. Hokama JY, Ritter LS, Davis-Gorman G, Cimetta AD, Copeland JG, McDonagh PF. Diabetes enhances leukocyte accumulation in the coronary microcirculation early in reperfusion following ischemia. *J Diabetes Complications* 2000; **14:** 96–107.
14. Shechter M, Merz CN, Paul-Labrador MJ, Kaul S. Blood glucose and platelet-dependent thrombosis in patients with coronary artery disease. *J Am Coll Cardiol* 2000; **35:** 300–307.
15. Title LM, Cummings PM, Giddens K, Nassar BA. Oral glucose loading acutely attenuates endothelium-dependent vasodilation in healthy adults without diabetes: An effect prevented by vitamins C and E. *J Am Coll Cardiol* 2000; **36:** 2185–2191.
16. Oswald GA, Smith CCT, Betteridge DJ, Yudkin JS. Determinants and importance of stress hyperglycemia in non-diabetic with myocardial infarction. *Br Med J* 1986; **293:** 917–922.
17. Norhammar A, Tenerz A, Nilsson G, Hamsten A, Efendic S, Ryden L, et al. Glucose metabolism in patients with acute myocardial infarction and no previous diagnosis of diabetes mellitus: A prospective study. *Lancet* 2002; **359:** 2140–2144.
18. Tenerz A, Norhammar A, Silveira A, Hamsten A, Nilsson G, Ryden L, et al. Diabetes, insulin resistance, and the metabolic syndrome in patients with acute myocardial infarction without previously known diabetes. *Diabetes Care* 2003; **26:** 2770–2776.
19. Halter JB, Beard JC, Porte D Jr. Islet function and stress hyperglycemia: Plasma glucose and epinephrine interaction. *Am J Physiol* 1984; **247:** E47–E52.
20. Shamoon H, Hendler R, Sherwin RS. Altered responsiveness to cortisol, epinephrine, and glucagon in insulin-infused juvenile-onset diabetics: A mechanism for diabetic instability. *Diabetes* 1980; **29:** 284–291.
21. Uusitupa MI, Mustonen JN, Airaksinen KE. Diabetic heart muscle disease. *Ann Med* 1990; **22:** 377–386.
22. Miyazaki C, Takeuchi M, Yoshitani H, Otani S, Sakamoto K, Yoshikawa J. Optimum hypoglycemic therapy can improve coronary flow velocity reserve in diabetic patients: Demonstration by transthoracic doppler echocardiography. *Circ J* 2003; **67:** 945–950.
23. Tamada H, Nishikawa H, Mukai S, Setsuda M, Nakamura M, Suzuki H, et al. Impact of diabetes mellitus on angiographically silent coronary atherosclerosis. *Circ J* 2003; **67:** 423–426.
24. Tosaki A, Engelman DT, Engelman RM, Das DK. The evolution of diabetic response to ischemia/reperfusion and preconditioning in isolated working rat hearts. *Cardiovasc Res* 1996; **31:** 526–536.
25. Iwakura K, Ito H, Ikushima M, Kawano S, Okamura A, Asano K, et al. Association between hyperglycemia and the no-reflow phenomenon in patients with acute myocardial infarction. *J Am Coll Cardiol* 2003; **41:** 1–7.

Appendices

*JACSS Principal Investigators (*chairperson)*

*Ogawa H (Kumamoto University), Asada Y (Miyazaki Medical College), Tei C (Kagoshima University), Kimura K (Yokohama City University Medical Center), Tsuchihashi K (Sapporo Medical University), Ishihara M (Hiroshima City Hospital), Miyazaki S, Yamagishi M, Ikeda Y (National Cardiovascular Center), Shirai M (Yamaguchi University), Hiraoka H (Osaka University), Inoue T (Oita National Hospital), Sonoda M (National Hospital Kyusyu Cardiovascular Center), and Saito F (Nihon University Surugadai Hospital).

JACSS Participating Institutions and Clinical Investigators

Honda T (Social Welfare Organization Imperial Gift Foundation Incorporated Saiseikai Kumamoto Hospital), Ogata Y (Japanese Red Cross Kumamoto Hospital), Saito T (Kumamoto Central Hospital), Hokamura Y (Kumamoto City Hospital), Mizuno Y (Kumamoto Kinoh Hospital), Miyagi H (Kumamoto National Hospital), Matsumura T (Labor Welfare Corporation Kumamoto Rosai Hospital), Tabuchi T (Yatsushiro Health Insurance General Hospital), Sakaino N (Amakusa Medical Center), Kimura K (Arao City Hospital), Obata K (Health Insurance Hitoyoshi General Hospital), Shimomura H (Fukuoka Tokushukai Medical Center), Matsuyama K (Social Insurance Ohmuta-Tenryoh Hospital), Nakamura N (Shinbeppu Hospital), Yamamoto N (Miyazaki Prefectural Nobeoka Hospital), Hase M (Sapporo Medical University School of Medicine), Matsuki T (Shinnittetsu Muroran General Hospital), Hashimoto A (Kushiro City General Hospital), Abiru M (Oji General Hospital), Matsuoka T (National Hospital Kyusyu Cardiovascular Center), Toda H, Ri S (Kagoshima City Hospital), Toyama Y, Yamaguchi H, Toyoshima S (Nanpuh Hospital), Torii H (Kagoshima Medical Association Hospital), Atuchi Y, Miyamura A (Tenyokai Chuo Hospital), Hamasaki S (Kagoshima University Faculty of Medicine), and Miyahara K (Shinkyo Hospital).

Atherosclerosis Found on Carotid Ultrasonography Is Associated With Atherosclerosis on Coronary Intravascular Ultrasonography

Toshiyasu Ogata, MD, Masahiro Yasaka, MD, Masakazu Yamagishi, MD, Osamu Seguchi, MD, Kazuyuki Nagatsuka, MD, Kazuo Minematsu, MD

Objective. Little has been reported on the relationship between left main coronary artery atherosclerosis and carotid ultrasonographic results. We evaluated the association between carotid and coronary atherosclerosis assessed by coronary intravascular ultrasonography (IVUS) in 45 patients. ***Methods.*** We counted the number of plaques with intima-media thickness (IMT) greater than or equal to 1.1 mm and calculated a plaque score by summing all plaque thicknesses. With the use of IVUS, the percent plaque area was calculated at the proximal, middle, and distal sites of the left main coronary artery. The maximum percent plaque area and mean percent plaque area of the 3 sites were also calculated. Relationships among the degree of left main coronary artery atherosclerosis and carotid atherosclerosis and vascular risk factors were evaluated. ***Results.*** The mean percent plaque area and maximum percent plaque area were increased in men and in patients with hypertension compared with women and those without hypertension ($P < .1$). Both the average of the maximum common carotid IMT and plaque number were correlated with both the mean percent plaque area and maximum percent plaque area ($P < .05$). Men, the presence of hypertension, and the average of the maximum common carotid IMT were correlated with both the mean percent plaque area and maximum percent plaque area by multiple linear regression analysis ($P < .05$). ***Conclusions.*** The average of the maximum common carotid IMT was significantly correlated with left main coronary artery atherosclerosis evaluated by IVUS. ***Key words:*** atherosclerosis; carotid arteries; coronary disease; ultrasonography.

Abbreviations
CAD, coronary artery disease; IMT, intima-media thickness; IVUS, intravascular ultrasonography

Received September 30, 2004, from the Cerebrovascular (T.O., M.Y.as., K.N., K.M.) and Cardiovascular (M.Yam., O.S.) Divisions, Department of Medicine, National Cardiovascular Center, Osaka, Japan. Revision requested October 18, 2004. Revised manuscript accepted for publication November 17, 2004.

This study was partially supported by a research grant from the Ministry of Health, Labor, and Welfare, Japan (15A-1).

Address correspondence and reprint requests to Toshiyasu Ogata, MD, Department of Medicine and Clinical Science, Kyushu University, Maidashi 3-1-1, Higashi-ku, Fukuoka 812-8582, Japan.
E-mail: togata@intmed2.med.kyushu-u.ac.jp

Several studies have identified a relationship between the presence of carotid artery disease and coronary artery disease (CAD). An autopsy study showed a strong correlation between the extent of carotid and coronary atherosclerosis.[1,2] Both arterial beds share risk factors that contribute to the progression of atherosclerosis.[3,4] Ultrasonography is used to assess the presence and extent of atherosclerosis in the carotid and coronary arteries. The carotid intima-media thickness (IMT) has been shown to be a good index of the presence and extent of CAD.[5–8] Also, there is evidence of a strong relationship between the presence of carotid plaques and coronary lesions.[9–12]

Patients with severe left main CAD are known to have a poor long-term prognosis.[13–15] Although coronary angiography is considered the criterion standard for the diagnosis of left main CAD, the degree of atherosclerosis is often underestimated by this method. In contrast, intravascular ultrasonography (IVUS) has been shown to be more accurate and sensitive than coronary angiography in identifying left main coronary artery lesions.[16] Although increased IMT on carotid ultrasonography has been used as a noninvasive marker for CAD, there have been few reports assessing the relationship between left main coronary artery atherosclerosis and carotid ultrasonographic results directly.

The aim of this study was to determine whether atherosclerosis detected in the carotid arteries by carotid ultrasonography was related to the extent of left main coronary artery atherosclerosis evaluated by IVUS.

Materials and Methods

Between November 1, 2000, and December 31, 2002, carotid ultrasonography was performed on 45 Japanese patients (40 men and 5 women; mean age ± SD, 60.8 ± 10.7 years; median age, 62 years) with CAD who also underwent coronary angiography. This study was approved by the Ethics Committee of our hospital. We obtained informed consent about coronary angiography and IVUS from all patients or their families. Coronary angiography was performed by a standard technique to assess the number of involved vessels.

If CAD of more than 1 vessel was detected on coronary angiography, IVUS studies were performed with a single-element 30-MHz, 2.9F or 3.2F intracoronary ultrasonographic catheter (Hewlett-Packard Company, Palo Alto, CA) (Figure 1). The IVUS transducer (30-40 MHz, 1800 rpm) was carefully advanced to the distal site of the patient's left main coronary artery, and the transducer was automatically pulled back (0.5 or 1.0 mm/s) by a motorized pullback device (Cardiovascular Imaging Systems/Boston Scientific, Natick, MA). Special care was taken to visualize the vessel lumen circularly rather than elliptically. If the lumen appeared elliptical, the transducer was repositioned as centrally as possible in the vessel. All images were recorded on super VHS videotape for subsequent analysis.

Ultrasonographic measurements were performed with an offline computer. The vessel lumen area was determined by tracing the leading edge of the intima. The external elastic membrane area was determined by tracing the leading edge of the second bright echo.[17] The percent plaque area was calculated as {(external elastic membrane area – lumen area)/external elastic membrane area} × 100. It was measured at proximal, middle, and distal sites. The maximum percent plaque area and mean percent plaque area of the 3 measurements were used in this study. Calcification of the left main coronary artery was considered present if there was high echo density with acoustic shadowing of the plaque.[12]

Carotid ultrasonography was carried out by experienced clinicians (T.O. and M.Yas.) using an Ultramark 9 HDI unit (Philips Medical Systems, Bothell, WA) with a linear array pulsed wave transducer operating at 5.0 to 10.0 MHz. Neither of them knew about the results of the IVUS study. The pulse repetition frequency was primarily 5000 Hz, and the low-pass filter was 50 Hz. Imaging was performed while the patients were lying in a supine position with their head turned away from the side being scanned and neck extended. The origin of the internal carotid artery was examined in longitudinal and transverse planes.

The IMT was evaluated by 2 calipers on the frozen frame of a suitable longitudinal image as the distance between the luminal-intimal interface and the medial-adventitial interface of the artery. We measured the maximum IMT of each

Figure 1. Representative IVUS image of the left main coronary artery.

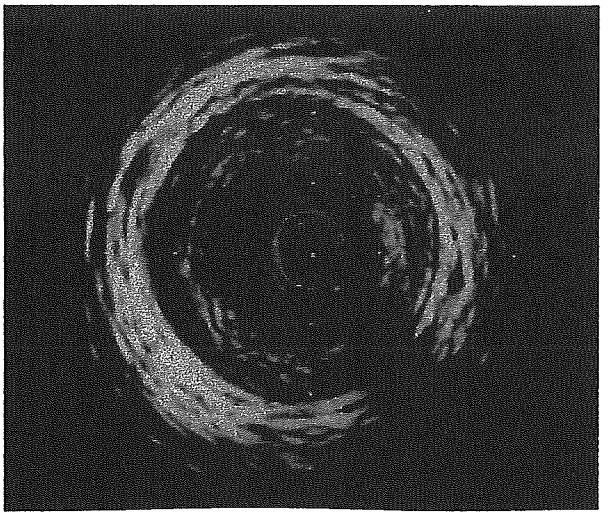

side of the common carotid artery and calculated their average (the average of the maximum common carotid IMT). We also measured the maximum IMT from the common carotid artery to the internal carotid artery on each side and averaged the results (the average of the maximum IMT). An atheromatous plaque was defined as a lesion with an IMT greater than or equal to 1.1 mm. We calculated plaque number by counting the numbers of plaques in both carotid arteries. To assess the severity of atherosclerosis, we used plaque score, which was calculated by summing all plaque thicknesses in both carotid systems.[18]

To examine the influence of patients' age on the percent plaque area, we divided them into 2 groups in the boundary of their median age (>62 and <62 years old). Hypertension was defined as systolic blood pressure greater than 140 mm Hg, diastolic blood pressure greater than 90 mm Hg, or current use of antihypertensive agents. Diabetes mellitus was defined as a hemoglobin A1C concentration greater than 6.5% or current use of hypoglycemic medications. Hypercholesterolemia was defined as total cholesterol concentration greater than 220 mg/dL or current use of cholesterol-lowering agents. Patients were categorized as smokers if they were current smokers.

The relationship between left main coronary artery atherosclerosis and carotid atherosclerosis was evaluated by simple linear regression analysis. Data were analyzed by StatView for Windows, version 5.0 (SAS Institute Inc, Cary, NC). The association between age, sex, presence of vascular risk factors, and percent plaque area in the left main coronary artery was examined by an unpaired t test. Multiple linear regression analyses were performed to determine atherosclerotic risk factors and carotid artery measurements that were significantly related to left main coronary artery atherosclerosis.

Results

The numbers of patients with hypertension, diabetes mellitus, and hypercholesterolemia and who were current smokers were 27 (60%), 21 (46.7%), 26 (57.8%), and 21 (46.7%), respectively. According to coronary angiography, 1-vessel disease was observed in 18 patients; 2-vessel disease was observed in 15 patients; and 3-vessel disease was observed in 12 patients. The mean percent plaque area ± SD was 34.1% ± 15.0%, and maximum percent plaque area was 37.5% ± 16.0%. The average of the maximum common carotid IMT, the average of the maximum IMT, plaque score, and plaque number were 0.98 ± 0.36 mm, 1.53 ± 0.88 mm, 4.26 ± 2.74 mm, and 2.4 ± 1.7, respectively. Significant differences in carotid ultrasonographic results were not observed among groups of patients with 1-, 2-, and 3-vessel disease.

There was no significant relationship between the mean percent plaque area, maximum percent plaque area, and patient's age (Table 1). The mean percent plaque area and maximum percent plaque area in men were increased significantly compared with those in women. The mean percent plaque area and maximum percent plaque area in patients with hypertension were also higher than those without hypertension. The mean percent plaque area and maximum percent plaque area did not differ statistically according to the presence of diabetes mellitus, hypercholesterolemia, or current smoking.

The average of the maximum common carotid IMT was correlated with both the mean percent plaque area and maximum percent plaque area on the basis of simple regression analysis (Table 2 and Figure 2). However, the average of the maximum IMT and plaque score did not significant-

Table 1. Mean and Maximum Percent Plaque Area by Patients' Clinical Characteristics

Characteristic	Mean %PA		Max %PA	
	Mean	*P*	Mean	*P*
Age				
<62 y	33.6		36.9	
>62 y	34.5	.85	37.9	.84
Sex				
Male	35.7		39.2	
Female	20.9	.036	23.5	.037
Hypertension				
Presence	38.3		40.9	
Absence	27.6	.017	32.3	.077
Diabetes mellitus				
Presence	31.0		34.4	
Absence	36.8	.20	40.2	.23
Hypercholesterolemia				
Presence	33.4		37.3	
Absence	34.9	.75	37.6	.95
Smoking habit				
Presence	34.6		39.0	
Absence	32.9	.73	32.9	.33

Max %PA indicates maximum percent plaque area; and Mean %PA, mean percent plaque area.

Table 2. Mean and Maximal Percent Plaque Area by Carotid Ultrasonographic Parameters

Parameter	Mean %PA		Max %PA	
	r	*P*	*r*	*P*
Max IMT-C avg, mm	0.39	.007	0.41	.005
Max-IMT avg, mm	0.14	.36	0.16	.30
PS, mm*	0.18	.22	0.22	.15
PN*	0.32	.034	0.35	.021

Max-IMT avg indicates average maximum IMT from the common carotid artery to the internal carotid artery on each side; Max IMT-C avg, average maximum IMT of each side of the common carotid artery; Max %PA, maximum percent plaque area; Mean %PA, mean percent plaque area; PN, plaque number; and PS, plaque score.
*Spearman rank correlation.

Figure 2. Scattergram of mean percent plaque area (mean %PA) and maximum percent plaque area (max %PA) by average maximum IMT of each side of the common carotid artery (max IMT-C avg). The max IMT-C avg was correlated with both mean %PA and max %PA on the basis of simple regression analysis (mean %PA: $r = 0.39$; $P = .007$; max %PA: $r = 0.41$; $P = .005$).

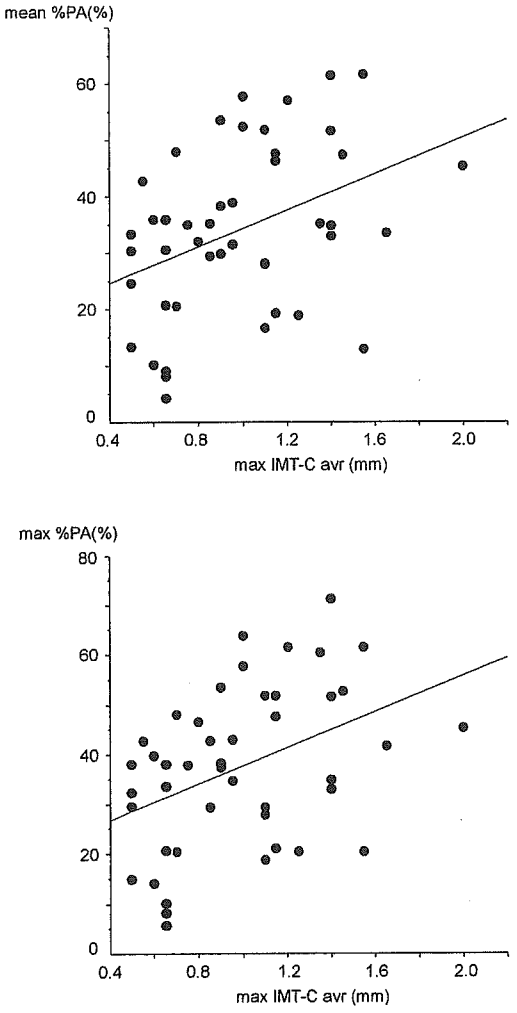

ly correlate with the mean percent plaque area or maximum percent plaque area. Plaque number was correlated with the mean percent plaque area and maximum percent plaque area (Figure 3). The average of the maximum common carotid IMT, average of the maximum IMT, plaque score, and plaque number of patients with calcifications in the left main coronary artery did not differ from those without calcifications.

All clinical and carotid ultrasonographic parameters with a significant relationship with the mean percent plaque area and maximum percent plaque area were tested with multivariate analysis (Table 3). Male sex, patients with hypertension, and the average of the maximum common carotid IMT were correlated with both the mean percent plaque area and maximum percent plaque area.

Figure 3. Scattergram of mean percent plaque area (mean %PA) and maximum percent plaque area (max %PA) by plaque number (PN). The PN was correlated with both mean %PA and max %PA on the basis of Spearman rank correlation (mean %PA: $r = 0.32$; $P = .034$; max %PA: $r = 0.35$; $P = .021$).

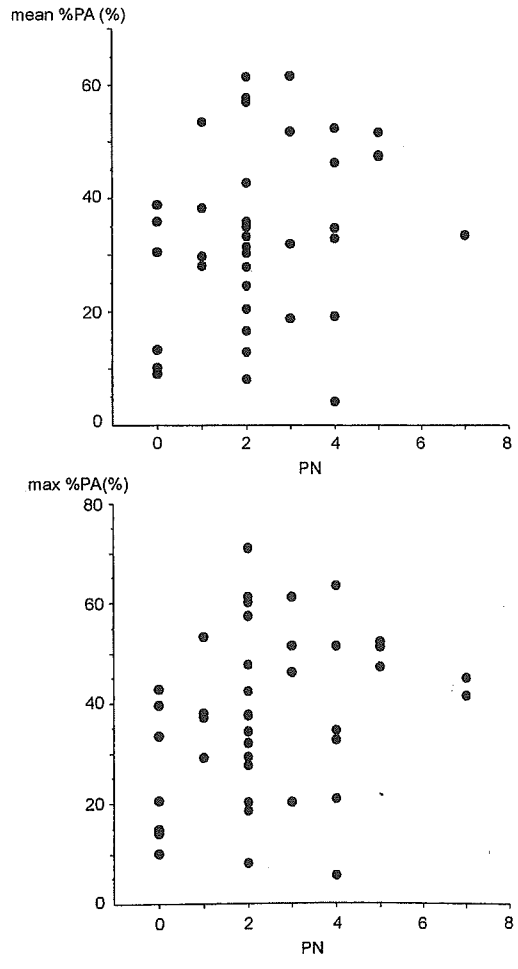

Table 3. All Clinical and Carotid Ultrasonographic Parameters and Relationship With Mean and Maximum Percent Plaque Area in the Multivariate Analysis

Parameter	Mean %PA		Max %PA	
	β	*P*	β	*P*
Male	0.37	.005	0.35	.010
Hypertension	0.46	.003	0.36	.021
Max IMT-C avg	0.50	.006	0.51	.008
PN	−0.24	.21	−0.21	.30

Max IMT-C avg indicates average maximum IMT of each side of the common carotid artery; Max %PA, maximum percent plaque area; Mean %PA, mean percent plaque area; and PN, plaque number.

Discussion

It has been reported that the IMT of the carotid artery is related not only to the presence of CAD but also to the occurrence of coronary events[5–8,19,20] There have been few reports concerning the relationship between carotid and left main coronary artery stenosis in patients undergoing coronary angiography.[21] Coronary angiography significantly underestimates the presence of atherosclerotic stenosis in the left main coronary artery because of coronary remodeling and methodological limitations.[16,22–24] Conversely, because IVUS permits detailed, high-quality cross-sectional imaging of the coronary arteries in vivo, we can evaluate the precise extent of left main coronary artery atherosclerosis. This study showed that the average of the maximum common carotid IMT, a parameter of carotid ultrasonographic findings, was correlated with accurate measurements of left main coronary artery atherosclerosis. It is well known that left main CAD is related to a patient's prognosis. Therefore, this carotid ultrasonographic finding may be associated with long-term prognosis. However, more research is needed on the correlation between the degree of carotid atherosclerosis and long-term prognosis.

A limitation of this study was that all patients had CAD. This selection bias meant that our findings regarding the relationship between carotid disease and left main CAD are relevant only to this specific group of patients and may not be applied to the general population.

Hypercholesterolemia and diabetes mellitus are known as important risk factors for the development of coronary atherosclerosis in Japan. In this study, however, male sex and hypertension were independent predictive factors rather than hypercholesterolemia and diabetes mellitus because all patients had CAD.

In conclusion, left main coronary artery atherosclerosis seems to be correlated with the average of the maximum common carotid IMT assessed by carotid ultrasonography as well as with men and the presence of hypertension. The average of the maximum common carotid IMT is the most important carotid ultrasonographic factor associated with left main coronary artery atherosclerosis.

References

1. Young W, Gofman JW, Tandy R. The quantification of atherosclerosis? The extent of correlation of degrees of atherosclerosis within and between the coronary and cerebral vascular beds. Am J Cardiol 1960; 6:300–308.
2. Mitchell JRA, Schwartz CJ. Relationship between arterial disease in different sites: a study of the aorta and coronary carotid and iliac arteries. Br Med J 1962; 5288:1293–1301.
3. Geroulakos G, O'Gorman D, Nicolaides A, Sheridan D, Elkeles R, Shaper AG. Carotid intima-media thickness: correlation with the British Regional Heart Study risk score. J Intern Med 1994; 235:431–433.
4. Persson J, Formgren J, Israelsson B, Berglund G. Ultrasound-determined intima-media thickness and atherosclerosis: direct and indirect validation. Arterioscler Thromb 1994; 14:261–264.
5. Geroulakos G, O'Gorman DJ, Kalodiki E, Sheridan DJ, Nicolaides AN. The carotid intima-media thickness as a marker of the presence of severe symptomatic coronary artery disease. Eur Heart J 1994; 15:781–785.
6. Crouse JR III, Craven TE, Hagaman AP, Bond MG. Association of coronary disease with segment-specific intimal-medial thickening of the extracranial carotid artery. Circulation 1995; 92:1141–1147.
7. Sugo A, Nakajima S, Kurata T, Mokuno H, Daida H, Yamaguchi H. Ultrasonographic assessment of carotid atherosclerosis emphasizing the variety of intimal-medial thickness and the relationship with coronary risk factors. J Cardiol 1997; 30:321–329.

8. Balbarini A, Buttitta F, Limbruno U, et al. Usefulness of carotid intima-media thickness measurement and peripheral B-mode ultrasound scan in the clinical screening of patients with coronary artery disease. Angiology 2000; 51:269–279.

9. Wofford JL, Kahl FR, Howard GR, McKinney WM, Toole JF, Crouse JR III. Relation of extent of extracranial carotid artery atherosclerosis as measured by B-mode ultrasound to the extent of coronary atherosclerosis. Arterioscler Thromb 1991; 11:1786–1794.

10. Craven TE, Ryu JE, Espeland MA, et al. Evaluation of the associations between carotid artery atherosclerosis and coronary artery stenosis: a case-control study. Circulation 1990; 82:1230–1242.

11. Bruckert E, Giral P, Salloum J, et al. Carotid stenosis is a powerful predictor of a positive exercise electrocardiogram in a large hyperlipidemic population. Atherosclerosis 1992; 92:105–114.

12. Giral P, Bruckert E, Dairou F, et al. Usefulness in predicting coronary artery disease by ultrasonic evaluation of the carotid arteries in asymptomatic hypercholesterolemic patients with positive exercise stress tests. Am J Cardiol 1999; 84:14–17.

13. Conti CR, Selby JH, Christie LG, et al. Left main coronary artery stenosis: clinical spectrum, pathophysiology, and management. Prog Cardiovasc Dis 1979; 22:73–106.

14. Lim JS, Proudfit WL, Sones FM Jr. Left main coronary arterial obstruction: long-term follow-up of 141 nonsurgical cases. Am J Cardiol 1975; 36:131–135.

15. Takaro T, Peduzzi P, Detre KM, et al. Survival in subgroups of patients with left main coronary artery disease: Veterans Administration Cooperative Study of Surgery for Coronary Arterial Occlusive Disease. Circulation 1982; 66:14–22.

16. Ge J, Liu F, Gorge G, Haude M, Baumgart D, Erbel R. Angiographically "silent" plaque in the left main coronary artery detected by intravascular ultrasound. Coron Artery Dis 1995; 6:805–810.

17. Kawano S, Yamagishi M, Hao H, Yutani C, Miyatake K. Wall composition in intravascular ultrasound layered appearance of human coronary artery. Heart Vessels 1996; 11:152–159.

18. Handa N, Matsumoto M, Maeda H, Hougaku H, Kamada T. Ischemic stroke events and carotid atherosclerosis: results of the Osaka Follow-up Study for Ultrasonographic Assessment of Carotid Atherosclerosis (the OSACA Study). Stroke 1995; 26:1781–1786.

19. del Sol AI, Moons KG, Hollander M, et al. Is carotid intima-media thickness useful in cardiovascular disease risk assessment? The Rotterdam Study. Stroke 2001; 32:1532–1538.

20. Hodis HN, Mack WJ, LaBree L, et al. The role of carotid arterial intima-media thickness in predicting clinical coronary events. Ann Intern Med 1998; 128:262–269.

21. Kallikazaros I, Tsioufis C, Sideris S, Stefanadis C, Toutouzas P. Carotid artery disease as a marker for the presence of severe coronary artery disease in patients evaluated for chest pain. Stroke 1999; 30:1002–1007.

22. Yamagishi M, Hongo Y, Goto Y, et al. Intravascular ultrasound evidence of angiographically undetected left main coronary artery disease and associated trauma during interventional procedures. Heart Vessels 1996; 11:262–268.

23. Hermiller JB, Buller CE, Tenaglia AN, et al. Unrecognized left main coronary artery disease in patients undergoing interventional procedures. Am J Cardiol 1993; 71:173–176.

24. Gerber TC, Erbel R, Gorge G, Ge J, Rupprecht HJ, Meyer J. Extent of atherosclerosis and remodeling of the left main coronary artery determined by intravascular ultrasound. Am J Cardiol 1994; 73:666–671.

Intravascular Shear Stress Imaging Based on Ultrasonic Velocity Vector Measurement

Naotaka Nitta[1], Kazuhiro Homma[1] and Tsuyoshi Shiina[2]

1)National Institute of Advanced Industrial Science and Technology (AIST), Tsukuba 305-8564, Japan
2)Graduate School of Systems and Information Engineering, Univ. of Tsukuba, Tsukuba 305-8573, Japan

Abstract - It has been reported that the wall shear stress affects the biochemical function of endothelial cell and the development of arteriosclerosis plaque. Therefore, the quantitative estimation of the wall shear stress has possibilities to be useful for the prevention of arteriosclerosis. In this paper, a novel method for the real-time and quantitative estimation of intravascular shear stress distribution is proposed based on the estimates of the viscosity and the shear rate distribution.

Experimental investigation, in which two types of fluids with different viscosity coefficient (water, and water mixed by PVA) flowed at a constant flow rate in a silicone tube with a simulated arteriosclerosis plaque, was performed. After estimating the viscosity coefficient and the shear rate distribution based on the ultrasonic measurements of the velocity vector distribution in the tube, the shear stress distributions were obtained. The averaged value of the shear stress distribution estimated in the higher viscosity fluid (water mixed by PVA: 0.3 Pa) became larger than that in the lower viscosity fluid (water: 0.1 Pa). These results reveal that the proposed method is technically valid for the quantitative shear stress estimation.

I. INTRODUCTION

Relationships between the intravascular wall shear stress, which is controlled by both viscosity of blood and flow dynamics, and the development of arteriosclerosis plaque have been clarified by various researches. Some evidences, which support the hypothesis that the arteriosclerosis plaque occurs frequently at the intimal regions stimulated by the low shear stress or the oscillatory shear stress, are reported [1]. Furthermore, the influences of the shear stress to the vulnerable plaque rupture are also reported [2]. On the other hand, it is also reported that the wall shear stress affects the biochemical function of endothelial cell such as the production of nitric oxide (NO) which has an anti-arteriosclerosis effect [3]. Therefore, various researches have been investigated the shear stress assessment since it might be useful for the prevention of arteriosclerosis.

The methods for assessing the wall shear stress noninvasively are classified by two methodologies. One method is based on the computational mechanics, in which the 3-D vascular reconstruction using various modalities (X-ray CT, MRI, IVUS and angiography) and the computational fluid dynamics (CFD) are combined for obtaining the intravascular shear stress distribution [4]. The other method is based on the velocity profile measurements by MRI and ultrasound, in which the shear rate is evaluated by spatially differentiating the velocity profile along the radial direction [5], or the shear stress is obtained by the multiplication of the calculated shear rate and the predetermined viscosity coefficient, in which the viscosity coefficient is preliminarily measured by using blood sample after the drawing [6]. Most techniques evaluate the shear rate or the shear stress with the predetermined viscosity because the viscosity coefficient changes due to non-Newtonian property of blood. However, when the shear stress is defined by the Newton's law of viscosity, the local variation of viscosity coefficient might affect the quantitative shear stress estimation. Therefore, if a novel technique for the local shear stress assessment can be established by considering the viscosity assessment, it is expected to be a more quantitative shear stress assessment technique.

So far, in order to evaluate the blood characteristics as typified by its viscosity, we have investigated a method for estimating the kinematic viscosity coefficient based on the ultrasonic blood flow measurement [7]. In this study, by extending the method for kinematic viscosity estimation to the shear stress estimation, a novel method for the real-time and quantitative estimation of intravascular shear stress distribution is proposed.

Technical validity of the method was investigated by conducting the preliminary flow-phantom experiment.

II. SHEAR STRESS IMAGING

Base on the Newton's law of viscosity, the shear stress can be defined by multiplying the shear rate by the viscosity coefficient. Therefore, if both of the viscosity coefficient and the shear rate can be obtained, the shear stress can be attained quantitatively. Based on the definition, the most classic assessment for the shear stress is a method which obtains the shear stress based on the assumption of Hagen-Poiseuille flow in a rigid circular tube. It is well known that the shear stress based on the Hagen-Poiseuille assumption is quite different from the actual shear stress because the idealized assumption cannot adapt to the actual in vivo vascular structure.

In this paper, it is assumed that blood is an isotropic, incompressible and linear viscous fluid, or that the blood property at the phase in the pulsation is approximated as the Newtonian fluid. Assuming that the velocity vector distribution can be obtained in the flow field with vorticity, the kinematic viscosity coefficient v can be estimated as follows, by eliminating the pressure terms in the Navier-Stokes equations with the differential operations [7].

$$v = \frac{\frac{D\xi}{Dt} - \left(\varsigma\frac{\partial}{\partial x} + \eta\frac{\partial}{\partial y} + \xi\frac{\partial}{\partial z}\right)w}{\nabla^2\xi} \qquad (1)$$

where (ξ, ς, η) and (u, v, w) indicate the vorticity components and the velocity vector components, and these relationships are defined as $\xi = \partial v/\partial x - \partial u/\partial y$, $\varsigma = \partial w/\partial y - \partial v/\partial z$ and $\eta = \partial u/\partial z - \partial w/\partial x$, respectively. In this paper, the above 3-D version in a xyz space is approximated by the 2-D version on x-y plane shown in eq.(2) because of the technical limitation of the ultrasonic velocity vector measurement.

$$v = \frac{\frac{\partial\xi}{\partial t} + u\frac{\partial\xi}{\partial x} + v\frac{\partial\xi}{\partial y}}{\frac{\partial^2\xi}{\partial x^2} + \frac{\partial^2\xi}{\partial y^2}} \qquad (2)$$

The above equations indicate that the kinematic viscosity coefficient can be obtained by the velocity vector distribution alone.

Next, the shear stress distribution on the x-y plane is estimated based on eq. (3).

$$\tau_{xy} = \mu\left(\frac{\partial u}{\partial y} + \frac{\partial v}{\partial x}\right) \qquad (3)$$

where μ ($= \rho v$, ρ : density) is the viscosity coefficient. Since the kinematic viscosity coefficient is defined as the ratio of the viscosity coefficient to the density, the shear stress can be obtained by converting the kinematic viscosity coefficient v into the viscosity coefficient μ under the assumption that the density is known. That is, while the conventional method uses the predetermined viscosity coefficient, the proposed method estimates the kinematic viscosity coefficient and uses the predetermined density. The advantage for the use of the predetermined density is exemplified in the experiment.

The estimate of the shear stress distribution based on eq.(3) needs the 2-D velocity vector distribution. In this paper, the ultrasonic blood flow measurement by Doppler method is utilized. However, Doppler method can obtain the only beam-axis component (v) of the velocity vector. Therefore, the lateral component (u) of the velocity vector was estimated based on the incompressible condition as follows.

$$u = -\int_{x_0}^{x}\frac{\partial v}{\partial y}dx + u_0 \qquad (4)$$

where u_0 is the initial value of the lateral velocity component provided by the angular correction of the measured beam-axis velocity component. Practically, the lateral velocity component is estimated by the iterative method [7].

III. EXPERIMENTAL SETUP

In order to empirically investigate the validity of the proposed method, an experimental setup is constructed as shown in Fig.1. A silicone tube with a diameter of 5 mm was immersed in a water tank. A step simulating the arteriosclerosis plaque (hemispherical step, width: 5 mm, height: 2 mm) was attached on the inner tube wall within the region of interest (ROI) to create the velocity vector field with vorticity, which is needed for estimating the kinematic viscosity coefficient. The ultrasonic probe driven at a center frequency of 4.7 MHz was set on the top of the central tube axis within ROI, a set of successive echo data for the estimate of 2-D velocity vector distribution were acquired by transmitting 74 pulses at each scan line. The scan line numbers for constructing one frame were 20, and the

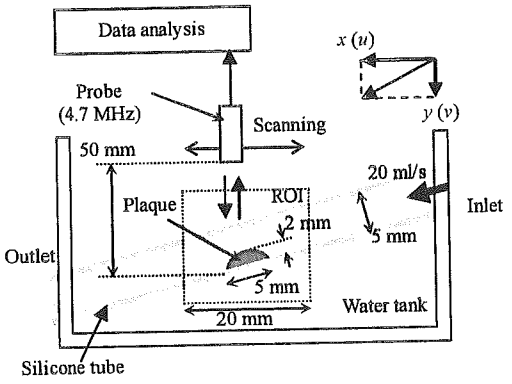

Fig.1 Experimental setup.

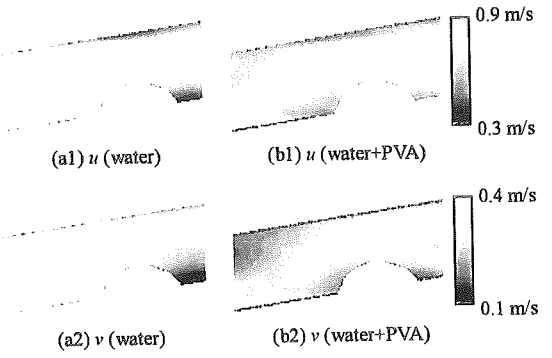

Fig.2 Estimated results of velocity vector components.

angle between the ultrasonic beam and the central tube axes was set to 67° . In order to investigate the possibility for detecting the differences of the shear stress between fluid types by the proposed method, two types of fluids with the different viscosity coefficient (one is water, and the other is water mixed by polyvinyl alcohol (PVA); both fluids include the scattering source) were flowed at a constant flow rate (20 ml/s) in the silicone tube under the constant temperature (21° C). The aim of this experiment is to verify the technical validity of the proposed method by using these fluids whose viscosity can be easily and stably controlled. Here, the viscosity coefficient increases by mixing PVA into water. Therefore, the viscosity coefficient of water mixed by PVA can be approximated to that of the actual blood (about 3 mPa·s) by adjusting the volume of PVA.

After data acquisition, following procedures were performed.

(1) Estimate of the 2-D velocity vector distribution based on eq.(4).
(2) Estimate of the kinematic viscosity coefficient based on eq.(2) and conversion into the viscosity coefficient by using the predetermined density.
(3) Shear rate calculation by differentiating 2-D velocity vector distribution.
(4) Estimate of the shear stress distribution based on eq.(3).

IV. RESULTS AND DISCUSSIONS

Figure 2 shows the estimated distributions of the 2-D velocity vector components where the strong echoes from the tube wall and the step are removed. Valid distributions that the flow speed becomes fastest at the top of the stenosis were appeared, and the variations of

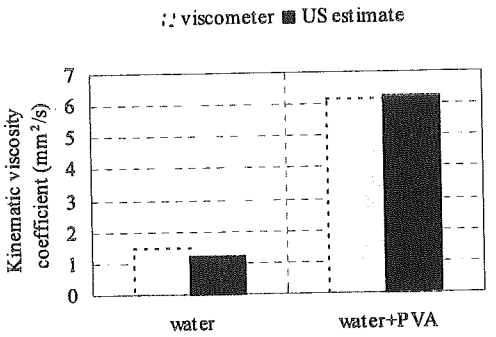

Fig.3 Comparison of the kinematic viscosity coefficients estimated by the proposed method and the viscometer.

flow state due to the differences of viscosity coefficients were also observed.

The kinematic viscosity coefficients were estimated by substituting the estimated 2-D velocity vector distributions as shown in Fig.2 into eq. (2). In addition, the kinematic viscosity coefficient was regarded as a constant value in fluid, and it was estimated by using the velocity vector around the step in which the vorticity exists. Figure 3 shows the comparisons of the kinematic viscosity coefficient between the estimated results by the proposed method and the measured results by the viscometer. The averaged error of the estimated values by the proposed method to the measured values by the viscometer was 9 %. From these results, the validity of the kinematic viscosity estimation was verified.

Finally, the shear stress distributions were obtained as shown in Fig.4. Here, the estimated kinematic viscosity coefficient was converted to the viscosity coefficient by assuming the density of 1.0 g/ml, and the shear rate distributions were calculated by the central difference

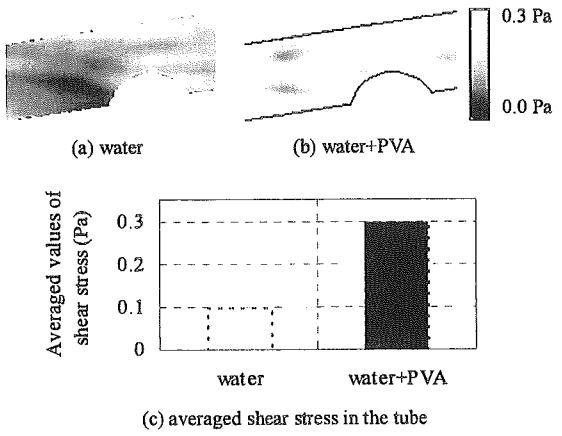

Fig.4 Shear stress imaging and the comparison between two types of fluids.

Table 1 Comparison of the density, the viscosity coefficient and the kinematic viscosity coefficient.

	water	water+PVA	ratio
density (g/ml)	1.02	1.05	1.03
viscosity coefficient (mPa·s)	1.57	6.47	4.12
kinematic viscosity coefficient (mm^2/s)	1.54	6.16	4

operation after smoothing of each distribution of the velocity vector components. In general, the magnitude of the shear stress distribution in a tube becomes largest near the tube wall. Figure 4 reflects the tendency of the common shear stress distribution. In addition, since the experiments were performed under a constant flow rate, the wall shear stress in water mixed by PVA which exhibits the higher viscosity is larger than that in water which exhibits the lower viscosity. Since the averaged shear stress in water is 0.1 Pa and that in water mixed by PVA is 0.3 Pa, the estimated shear stresses reflect the differences of viscosity and are valid. Table 1 shows the comparisons among the density, the viscosity coefficient and the kinematic viscosity coefficient of water and water mixed by PVA, respectively. In water and water mixed by PVA, the ratios of viscosity coefficient and kinematic viscosity coefficient are larger than the ratio of the density. The kinematic viscosity coefficient is strongly influenced of the viscosity coefficient, not the density. Therefore, under such situation, while there is a risk that it might become impossible for the difference in shear stress to be quantitatively detected if the viscosity coefficient is predetermined, the proposed method can attain more quantitative shear stress distribution.

V. CONCLUSIONS

In this study, a novel method for estimating the intravascular shear stress distribution was proposed by considering the estimate of the viscosity coefficient. Experimental results revealed the technical validity of the proposed method.

The ultimate aim is to evaluate the intravascular shear stress distribution more accurately and quantitatively. In future work, the improvement of accuracy for velocity vector measurement, the effective removal of the clutter components during pulsation, and the selection of the appropriate pulsation phase for valid estimation will be investigated for achieving the ultimate goal.

REFERENCES

[1] A.M. Shaaban, A.J. Duerinckx: Wall shear stress and early atherosclerosis - A review. AJR Am J Roentgenol. **174** (6): 1657-1665, 2000.

[2] E. Falk, P.K. Shah, V. Fuster: Coronary plaque disruption. Circulation. **92**: 657-671, 1995.

[3] J. Hanjoong; C.B. Yong: Shear stress regulates endothelial NO synthase (eNOS) by the protein kinase A (PKA)-dependent mechanisms. Proc. of 2002 EMBS/BMES conf. **1**: 639-640, 2002.

[4] R. Krams, J.J. Wentzel, J.A. Oomen: Evaluation of endothelial shear stress and 3D geometry as factors determining the development of atherosclerosis and remodeling in human coronary arteries in vivo - Combining 3D reconstruction from angiography and IVUS (AN-GUS) with computational fluid dynamics. Arterioscler Thromb Vasc Biol. **17** (10): 2061-2065, 1997.

[5] G. Bambi; T. Morganti; S. Ricci; F. Guidi; P. Tortoli: Real-time simultaneous assessment of wall distension and wall shear rate in carotid arteries. Proc. of 2004 IEEE Int Ultrason Symp.: 592-595, 2004.

[6] S.P. Wu, S. Ringgarrd, E.M. Pedersen: Three-dimensional phase contrast velocity mapping acquision impromes wall shear stress estimation in vivo. Mag Res Imag. **22** (3): 345-351, 2004.

[7] N. Nitta, K. Homma: Ultrasonic measurement of fluid viscosity for blood characterization. Jpn J Appl Phys. **44** (6B): 4602-4608, 2005.

PROCEEDINGS

of the
Fourth International Conference
on the Ultrasonic Measurement and Imaging
of Tissue Elasticity©

Lake Travis, Austin, Texas, USA
October 16–19, 2005

Table of Contents

012 **PRELIMINARY RESULTS OF ELASTICITY IMAGING TO AORTIC PLAQUE.**

Takashi Osaka[1], Takeshi Matsumura[1], Tsuyoshi Mitake[1], Satoshi Nakatani[2], Tsuyoshi Shiina[3].*
[1]Research and Development Center, Hitachi Medical Corporation, Chiba, JAPAN; [2]Cardiology Division, National Cardiovascular Center, Osaka, JAPAN; [3]Graduate School of Systems and Information Engineering, University of Tsukuba, Ibaraki, JAPAN.

Background and Aims: In general, it is well known that cancer tissue becomes harder compared with other normal tissues. Our group has developed a real-time tissue elastography imaging system and continued to evaluate its clinical usefulness for application to organs such as the mammary gland, the prostate, the thyroid and other areas. In this paper, we report preliminary clinical results for aortic plaque.

Methods: RF image frames are transferred from the ultrasound scanner to an external PC, and these data frames are reconstructed into elasticity (strain) images with about 12 fps throughput on the PC. Additional signal and image processing is also accomplished in the PC in off-line mode. Strain images are obtained by differentiating displacements between neighboring frames. A special feature of the reconstruction algorithm that we use is based upon the "Combined Autocorrelation Method", that is, inter-frame displacements greater than a wavelength are estimated by envelope correlation in addition to the usual precise autocorrelation method to detect change of phase [1].

For application to the aorta, a transesophageal echocardiography probe (TEE) is used to get RF image frames via the esophagus, and the variation of aortic blood pressure is used as the compression force without the need for any external compression devices.

The color-coded elasticity (strain) images are overlaid on the usual B-mode images in a translucent style. Here, harder areas are depicted in blue and softer areas in red, with intermediate hardness displayed in green.

System details:
- Ultrasound Scanner System: Hitachi EUB-8500
- External PC: Dell PowerEdge SC1420(3.2GHz Xeon Dual CPU Type)
- Probe: EUP-ES52M (Central Frequency 5.0MHz)

Preliminary Results: The patient was a 71 year old male. The plaque is about 2-3mm thick and is confined in the arrowed region in the transverse-axis B-mode TEE image. The corresponding tissue strain image obtained using our elastography system shows blue color in the arrowed region. This result suggests that the plaque might be a hard plaque and doesn't have potential for abrupt separation. This result encourages us to apply our system to more clinical study and also extend its application to other arterial diseases, e.g., arterial sclerosis.

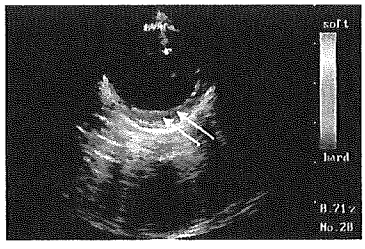

Figure1: Strain Imaging of Aortic Plaque

Reference:

[1] T. Shiina, M.M. Doyley, J.C. Bamber, "Strain Imaging Using Combined RF and Envelope Autocorrelation Processing", Proc. of 1996 IEEE Ultrasonics Symp. 1331-1336, 1997.

* *indicates Presenter*

循環器科，57(5)：435-439，2005

特集 心血管画像診断の新しい展開

血管内超音波エラストグラフィ*

椎名 毅**
山岸正和***

Key Words: intravascular ultrasound, elastography, vulnerable plaque, atherosclerotic plaque

はじめに

近年の研究成果により，不安定狭心症や急性心筋梗塞のほとんどはプラーク破綻(plaque rapture)を引き金とした血栓形成により，冠動脈内腔が狭窄および閉塞されて生じる急性疾患であることが明らかとなってきた．とくに，脂質が薄い線維被膜に覆われたプラークは破綻しやすい不安定プラークとなると考えられている[1]．したがって，この急性冠症候群の予防および治療には，プラークの安定度を決定している脂質，線維化，石灰化などの異なるプラーク組成を正確に識別し，プラークの安定度に関して適切な診断を下す必要がある．

一方で，組織性状は弾性と直接的な関係にあることが知られ，近年，癌などにより硬化した病変部の早期検出や進展範囲の同定を目的とした組織弾性イメージング法の研究が盛んに行われている[2)~6)]．

血管内エコー法(IVUS)においても，プラークのような組織性状が変化した領域を硬さの観点から捉える血管内超音波エラストグラフィ(IVUS elastography)の研究が注目されている[7)~15)]．

これは，拍動による血管壁の変形を利用して，硬い線維成分と軟らかい脂質成分などの組成が異なるプラークの性状を的確に把握しようとするもので，急性冠症候群の引き金となる不安定プラークの検出法のひとつとして注目されている．ここでは，血管内超音波エラストグラフィの原理と，臨床計測の実例を通して，プラーク性状評価への応用の現状と課題について概説してみたい．

血管内超音波エラストグラフィの原理

プラーク性状の相違は，軟らかい脂質や比較的硬い線維質などの組成の相違から，硬さ(弾性)の違いとして現れると予想される．血管径は拍動などにより変化するが，血管壁各部の歪み(局所的な伸縮率)は各部の弾性の違いに応じて異なる．破綻しやすい不安定プラークは，脂質性の柔らかい粥腫が薄い線維性の皮膜に覆われたものと考えられるが，これは，拍動による変形の大きな部位として捕らえることができる．血管内超音波エラストグラフィは，拍動による血管径が変化する過程において，隣接する2つのフレームについて，rfの超音波エコー信号を比較することで，図1に示すように，血管壁の各点(r, θ)の時刻tにおける変位ベクトル(v_r, v_θ)を計測する．ここで，$v_r(r, \theta, t)$，$v_\theta(r, \theta, t)$は，それぞれ半径方向，円周方向の変位を示す．

これまで，この局所変位を求める信号処理法

* Intravascular ultrasound elastography.

** Tsuyoshi SHIINA, M.D.: 筑波大学大学院システム情報工学研究科〔〒305-8573 つくば市天王台1-1-1〕; Graduate School of Systems and Information Engineering, University of Tsukuba, Tsukuba 305-8573, JAPAN
*** Masakazu YAMAGISHI, M.D.: 国立循環器病センター心臓血管内科部門

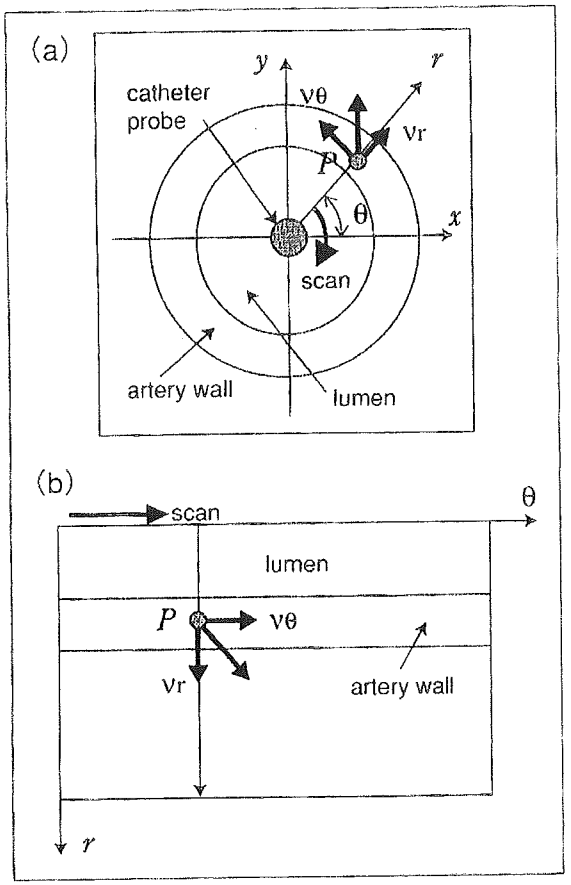

図1　血管断面における局所変位の計測

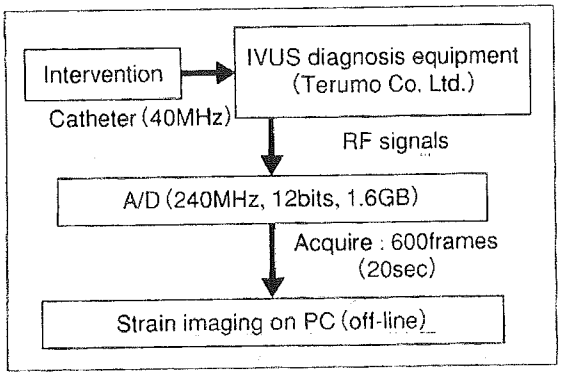

図2　血管超音波エラストグラフィ解析システム

としては，空間相関法[7]やドプラ法(自己相関法)[8][9]-[11]を応用した手法が提案されてきた．空間相関法は比較的大きな変位量を検出できるが，演算時間が多い点や誤ピークが多数出現する点で問題があり，一方，ドプラ法は高速に精度よく変位推定を行えるが，エイリアシングにより検出できる変位量が波長により制限を受ける点で問題があった．

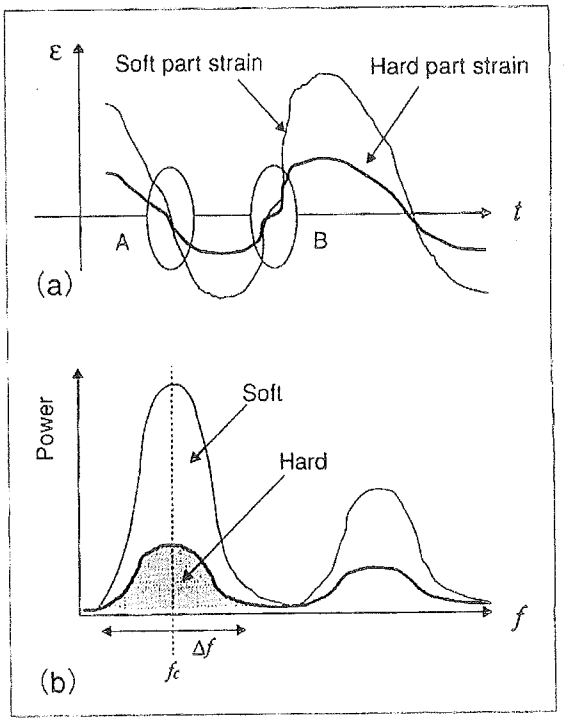

図3　ひずみの時間変動とストレインパワー算出

これに対して著者らは，空間相関法とドプラ法の利点を融合し，実際の臨床計測でみられるような波長以上の比較的大きな変位に対しても，高速かつ高精度に，安定した計測を可能とするCA法(複合自己相関法)を開発した[4][6]．さらに，IVUSプローブに対する血管の回転などの動きに対処するため，図1-bに示すような2次元探索を組み合わせることにより，測定精度の向上を図った．

この変位のうち，拍動による血管壁厚の変化を表す成分は半径方向の変位$v_r(r, \theta, t)$であるが，これ自体は血管全体の動きを含んでいるので，次式のように半径方向に空間微分することによって，局所的な変形率(ひずみ)$\varepsilon_r(r, \theta, t)$の分布を求める．

$$\varepsilon_r(r, \theta, t) = \frac{\partial v_r(r, \theta, t)}{\partial r} \quad \cdots\cdots\cdots\cdots (1)$$

このひずみは，当然，血圧による圧迫の強さにより変化するが，近傍での応力の変化が急峻でないとすれば，ひずみの大きな部分は変形しやすさを表すので，いわば硬さの分布を相対的に反映した量といえる．これに対し，もし，その点での半径方向と回転方向の応力分布(σ_r, σ_θ)

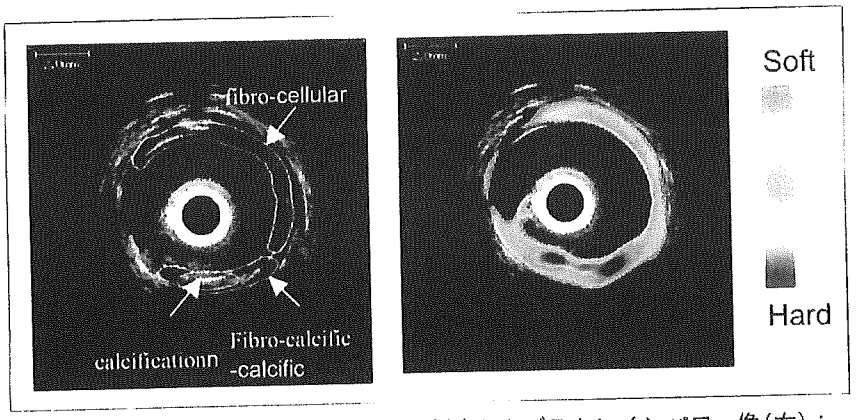

図4　冠動脈のIVUSによるBモード(左)およびストレインパワー像(右)：
複合したプラークを有する症例

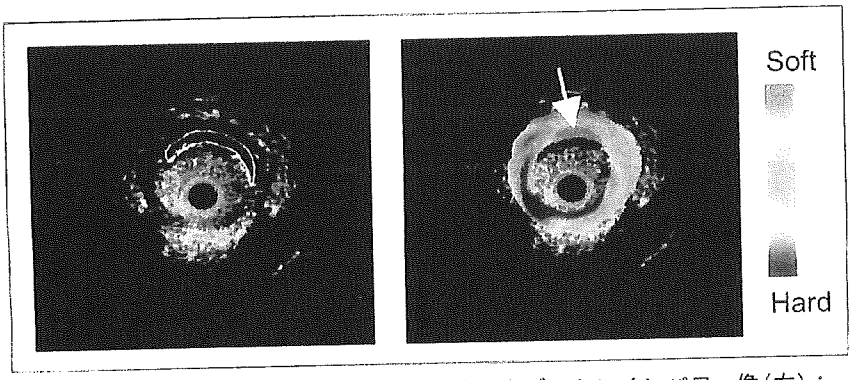

図5　冠動脈のIVUSによるBモード(左)およびストレインパワー像(右)：
脂質性の不安定プラークを有する症例

が得られれば，いくつかの近似のもとに，その点での弾性係数(ヤング率)が次式から推定できる[9]．

$$E=\frac{(1+\nu)\,|(1-\nu)\,\sigma_r-\nu\sigma_\theta|}{\varepsilon_r} \quad \cdots\cdots\cdots (2)$$

ここで，νはポアソン比を表す．

しかし，一般に，血管各部の応力の分布を厳密に求めるのは難しく，また処理時間もかかる点で，現時点では血管内膜面での値，すなわち血圧を代用したり，半径方向のみの動きを1次元近似したりすることが多い．

このため著者らは，まず，ひずみ分布をもとに不安定プラークの性状を評価する方法について検討し，医療機器メーカ〔(株)テルモ〕と共同で，臨床データを解析できる装置を開発した．これは，図2に示すように，中心周波数40MHzのIVUSプローブを用いて，通常の冠動脈インターベンション中に，rfでの超音波エコー信号を計測するため，240MHz, 12bitでA/D変換し，1.6GBの大容量のメモリを搭載したボードを内蔵している．これにより，連続して600フレーム(約20秒)のデータを取得でき，拍動の各時相における歪み分布の時間変化を観察可能とした．

一方でひずみは，図3-aに示すように拍動に伴う血圧変化により変動する．そこで，拍動による時相の影響を受けずに冠動脈壁やプラークの弾性を表す特徴量として，図3-bに示すように1心拍内における歪み値変動のパワーを算出し，その分布像を得るストレインパワー像を提案した．これにより，1心拍での平均的な変形率が安定に表示される[13)-15)]．

血管超音波エラストグラフィの実際

開発されたシステムは，臨床データの解析によりその有効性の評価を試みた．臨床データの取得は通常の冠動脈インターベンション中に行われるが，実施医療機関における倫理委員会での承認，および患者への十分なインフォームド

コンセントのもとに実施された．

図4は，線維化および石灰化したプラークを含む症例であり，左図はBモード像，右図はストレインパワー像をパワーの高値を柔らかい部分として赤に，低値を硬い部分として青でBモード像に重ねて表示してある．図4-左では，コントラストは十分ではないが，動画として観察すると，10時方向から5時方向にわたって軟らかい細胞成分を含む線維化，5時方向から7時方向にわたって硬い石灰化を含む線維化を生じている様子が推測できる．図4-右では，9時方向にガイドワイヤによる陰影がみられ，ストレインパワーを画像化歪みパワーの推定が困難となっているものの，細胞成分および石灰化を含む2つの線維化領域が明瞭なコントラストで識別できることがわかる．

以上の結果から，異なるプラーク組成が識別される可能性が示唆されたといえる．

次に図5は，脂質性不安定プラークの計測結果例を示す．同じく，左図は通常のBモード像，右図はそれにストレインパワーをカラー表示したものである．脂質性プラークが可動性の大きい領域として描出され，歪みパワー像などの組織弾性イメージングが不安定プラークを検出する手段として有望であることが確認された．

結　論

硬さに基づくプラークの組織性状の違いを，可視化する血管内超音波エラストグラフィの原理と，不安定プラーク性状評価への応用について示してきたが，変形性という間接であるが硬さの指標を画像化することで，脂質性プラークなどの不安定性を評価する手段となりうることが示された．一方で，易破綻性の指標としては，硬さそのものより，プラークでの角の部位など，変形性の高い部位であり，その意味ではより直接的である可能性も出てくる．

今後検討すべき点として，易破綻性と組織弾性および病理組織学的な対応づけが重要といえる．また，不安定プラークにおいて，とくに破綻しやすい部位の検出を可能とするためには，測定法としては，一層の高分解能化，血圧値を同時計測することによる定量化，さらにシミュレーション解析による線維性皮膜や脂質コアの力学的特性と実際の不安定性との関連の把握に努める必要があろう．

謝辞：本稿で紹介した研究内容の一部は，平成15, 16年度国立循環器病センター循環器病研究委託費（15公-5）および平成16年度厚生労働省科学研究費の補助を受けた．

文　献

1) 上田真喜子，斎藤　穎．急性冠症候群の病態生理から見た治療戦略．Medical Tribune 1999；32：26.
2) Ophir J, Cespedes I, Ponnekanti H, et al. Elastography : A quantitative method for imaging the elasticity of biological tissues. Ultrason Imaging 1991；13：111.
3) O'Donnell M, Skovoroda AR, Shapo BM, et al. Internal displacement and strain imaging using ultrasonic speckle tracking. IEEE Trans Ultrason Ferroelectr Freq Control 1994；41：314.
4) Shiina T, Doyley MM, Bamber JC. Strain imaging using combined RF and envelope autocorrelation processing. Proc IEEE Ultrasonics Symp 1997：1331.
5) 椎名　毅，新田尚隆，植野　映，ほか．複合自己相関法による実時間Tissue Elasticity Imaging．日本超音波医学会誌 1999；26：57.
6) Yamakawa M, Shiina T. Strain estimation using the extended combined autocorrelation method. Jpn J Appl Phys 2001；40：3872.
7) de Korte CL, Pasterkamp G, van der Steen AFW, et al. Characterization of plaque components with intravascular ultrasound elastography in human femoral and coronary arteries *in vitro*. Circulation 2000；102：618.
8) Shapo BM, Crowe JR, Skovoroda AR, et al. Displacement and strain imaging of coronary arteries with intraluminal ultrasound. IEEE Trans Ultrason Ferroelect Freq Contr 1996；43：234.
9) 田波治彦，椎名　毅，新田尚隆，ほか．血管内エコー法による血管壁弾性率分布のイメージング．日本音響学会講演論文集 1999：1127.
10) 椎名　毅，新田尚隆，山川　誠．血管内エコー法

による動脈壁組織性状の可視化—*in vivo*実験による検討—．日本音響学会講演論文集 2001：1267.

11) Shiina T, Nitta N, Yamagishi M. Coronary arteries characterization based on tissue elasticity imaging —*in vivo* assessment—. Proc IEEE Ultrasonics Symp 2002：1811.

12) 新田尚隆，椎名　毅，山岸正和．IVUSによる冠動脈壁組織性状診断—*in vivo*計測による試み—．第21回日本医用画像工学会大会抄録集 2002：296.

13) 新田尚隆，遠藤浩幸，椎名　毅，ほか．血管内エコー法を用いた冠動脈弾性イメージング．電子情報通信学会論文誌DII 2004；1 J87-DII：78.

14) Shiina T, Nitta N, Yamagishi M. A new method for determining vulnerable atherosclerotic plaque by intravascular ultrasound elasticity imaging. Imaging Vulnerable Atheroscle rotic Plaque—The Evolving of New Imaging Technique—, Abstract of the 68th annual scientific meeting of Japanese Circulation Society. SY3-5March 2004.

15) Shiina T, Nitta N, Endo MH, et al. Assessment of vulnerable coronary plaque by intravascular elasticity imaging. Proc of IEEE International Ultrasonics, Ferroelectrics, and Frequency Control 50th Anniversary Joint Conference, in printing, Montreall. August 2004.

*　　*　　*